

---

## MAGNETIC CONFINEMENT SYSTEMS

---

# Plasma Confinement in a Levitated Magnetic Dipole

J. Kesner\* and M. Mauel\*\*

\* Massachusetts Institute of Technology, Cambridge, Ma 02129

\*\* Columbia University, New York, N.Y. 10027

Received April 1, 1995

**Abstract**—Plasma confinement in the field of a levitated dipole offers many advantages for magnetic fusion. MHD stability is obtained from compressibility which utilizes the large flux tube expansion of a dipole field. Such a device could be high beta, steady state, and exhibit good confinement properties. The large flux expansion will ease the difficulty of the divertor design. The configuration is ideal for electron cyclotron heating and controlled convective flow patterns may provide a mechanism for fueling and ash removal.

### 1. INTRODUCTION

The dipole magnetic field is the simplest and most common magnetic field configuration in the universe. It is the magnetic far-field of a single, circular current loop, and it represents the dominate structure of the middle magnetospheres of magnetized planets and neutron stars. The use of a dipole magnetic field generated by a levitated ring to confine a hot plasma for fusion power generation was first considered by Akira Hasegawa after participating in the Voyager 2 encounter with Uranus [1]. Hasegawa recognized that the inward diffusion and adiabatic heating that accompanied strong magnetic and electric fluctuations in planetary magnetospheres represented a fundamental property of strongly magnetized plasmas not yet observed in laboratory fusion experiments. For example, it is well-known that global fluctuations excited in laboratory fusion plasmas result in rapid plasma and energy loss. In contrast, large-scale fluctuations induced by sudden compressions of the geomagnetic cavity (due to enhancements in solar wind pressure) or by unsteady convections occurring during magnetic substorms energize and populate the energetic electrons trapped in the Earth's magnetosphere [2]. The fluctuations induce *inward* particle diffusion from the magnetospheric boundary even when the central plasma density greatly exceeds the density at the edge. Hasegawa postulated that if a hot plasma having pressure profiles similar to those observed in nature could be confined by a laboratory dipole magnetic field, this plasma might also be immune to anomalous (outward) transport of plasma energy and particles.

The dipole reactor concept is based on the idea of generating pressure profiles near marginal stability for low-frequency magnetic and electrostatic fluctuations. From ideal MHD, marginal stability results when the pressure profile,  $p$  satisfies the adiabaticity condition,  $\delta(pV^\gamma) = 0$ , where  $V$  is the flux tube volume and  $\gamma = 5/3$ . From gyro kinetics, marginal stability results when  $\partial F(\mu, J, \psi)/\partial \psi = 0$  where  $F(\mu, J, \psi)$  is the particle dis-

tribution function,  $\mu$  is the adiabatic invariant,  $\mu = \epsilon_\perp/2B$ ,  $J$  is the parallel invariant,  $J = \oint v_\parallel dl$  and the flux,  $\psi$  is the third adiabatic invariant. The frequencies that correspond to these invariants are respectively  $\Omega_c$  the cyclotron frequency,  $\omega_b$ , the bounce frequency and  $\omega_d$  the curvature driven precessional drift frequency. Both of these conditions lead to dipole pressure profiles that scale with radius as  $r^{-20/3}$  while the adiabatic distribution function,  $F(\mu, J)$  also implies a density dependence of  $n_e \propto r^{-4}$  and a temperature dependence  $T \propto r^{-8/3}$ .

By levitating the dipole magnet in order to prevent end losses, conceptual reactor studies supported the possibility of a dipole fusion reactor [3, 4]. The dipole reactor concept is a radical departure from the better known toroidal-based magnetic fusion reactor concepts. For example, the most difficult problems for a tokamak reactor are the divertor heat dissipation, disruptions, steady state operation, and an inherently low beta limit. Furthermore, the tokamak is subject to neo-classical effects and micro-turbulence driven transport. The dipole concept provides a approach to fusion which solves these problems.

1. Divertor problem: The difficulty in spreading the heat load at the divertor plate is generic to concepts in which the magnetic flux is trapped within the coil system. By having the plasma outside of the confining coil the magnetic flux can be sufficiently expanded to substantially reduce divertor heat loads.

2. Major disruptions: A tokamak has a large amount of energy stored in the plasma current. The dipole plasma carries only diamagnetic current and is inherently free of disruptions. Experiments observe relaxation oscillations, reminiscent of tokamak ELMs, which relax the pressure gradients when they become too large.

3. Steady state: A tokamak is a pulsed device and current drive schemes that are required for steady oper-

ation appear to be costly. The dipole plasma is inherently steady state.

4. Beta limit: Tokamak stability depends on the poloidal field which is less than the toroidal field by  $B_p/B_T \sim 1/qA$  with  $q$  the edge safety factor and  $A$  the aspect ratio. For a dipole there is a critical pressure gradient that can be supported (due to the compressibility term in the interchange stability criterion) and for a sufficiently gentle pressure gradient the dipole plasma resides in an absolute energy well and is stable up to local beta values in excess of unity.

5. Transport and neoclassical effects: The trapping of particles in regions of bad curvature makes the tokamak susceptible to drift frequency range trapped particle driven turbulent transport. A dipole could, theoretically, show classical transport. In addition a tokamak has a “neoclassical” degradation of transport that derives from the drifts of particles off of the flux surfaces. In a dipole the drifts are toroidal and they define the flux surfaces.

The chief drawback of the dipole approach is the need for a levitated superconducting ring internal to the plasma. Although this provides a challenge to the engineering of the device recent advances in high temperature superconductors coupled with an innovative design concept of Dawson [5, 6] on the maintenance of an internal superconducting ring in the vicinity of a fusion plasma leads to the conclusion that this issue is technologically solvable.

Utilization of electron cyclotron resonance heating (ECRH) and pellet injection in a levitated dipole permits a unique heating approach for the creation of fusion grade plasmas. The combination of closed field lines and high beta makes the dipole an ideal geometry for creating a high beta, hot electron plasma by the application of ECRH. Such plasmas have been demonstrated in open field line mirror machines as well as in levitrons and in the non-levitated dipole (or so-called “terrella”) CTX experiment [7–10]. The density of the hot electron plasma is observed to be limited by microwave accessibility and the energy by relativistic detuning. Unlike ECRH mirror applications, the hot electrons created in a levitated dipole can only be lost by cross-field transport and if transport is close to classical the resulting loss rate will be small. The energy stored in the hot electron plasma can be transferred into a dense, thermal hydrogenic plasma by injecting pellets into the ECR heated plasma.

We conclude that the continued advances in the understanding of magnetospheric plasmas coupled with the development of the technology of gyrotrons and of pellet injectors provides the fusion community with a new and unique approach to creating fusion grade laboratory plasmas. In addition the development of high temperature superconductors and of new conceptual approaches to the cooling of an internal levitated superconducting coil provide a potential path for

a substantially improved approach to magnetic fusion energy production.

## 2. DIPOLE CONFIGURATION

Figure 1 which shows the magnetic flux contours and the mod-B surfaces for a laboratory-size levitated dipole facility [11]. The levitated ring has a major radius  $R_c$  and a minor radius  $a$ . The simplest vacuum chamber geometry would be a spherical tank and the last closed flux surface will be assumed to have a radius  $R_w$ . Typically  $R_w \geq 5R_c$  to permit a substantial reduction of plasma pressure. The plasma pressure will attain a peak value at a midplane radius of  $R_0$ . Between the ring surface (located at  $R = R_c + a$ ) and the peak pressure location there is good curvature and since the field is relatively high near the ring, cross-field transport is expected to be low. Thus we expect high pressure gradients in this region. The schematic midplane pressure profile is shown in Fig. 2.

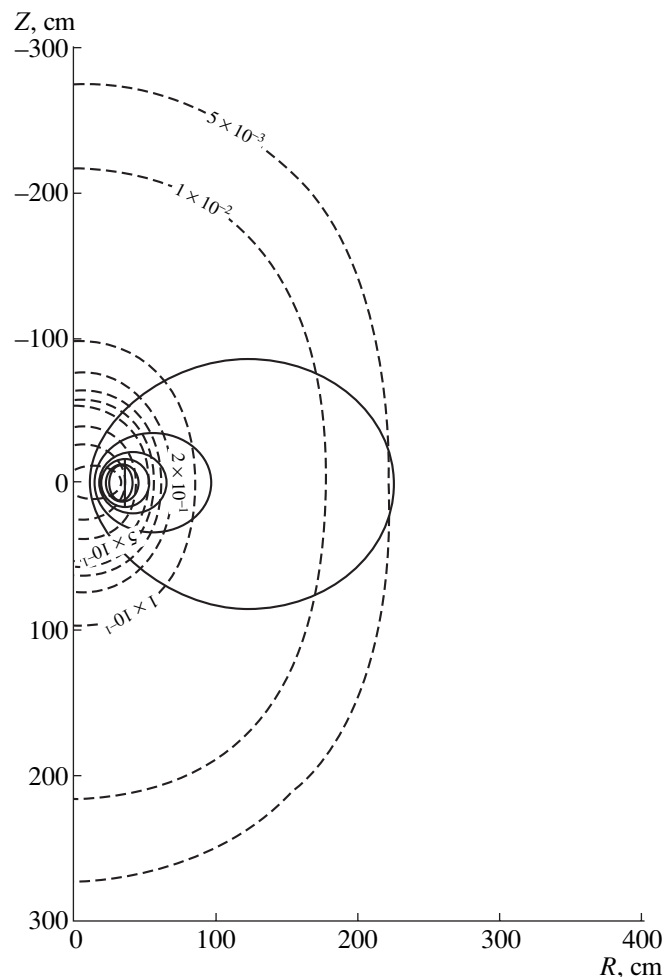


Fig. 1. Magnetic field and flux surfaces for a levitated dipole experiment.

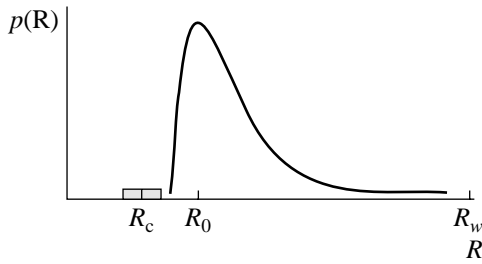


Fig. 2. Midplane pressure profile shown schematically.

Outside of the peak pressure region the pressure will decay in a region of “bad” curvature and MHD stability requires a relatively gentle pressure gradient. This results in a large volume of low field and of low density plasma. Thus a dipole confinement device would look like a small ring surrounded by a hot plasma that is centered within a relatively large spherical vacuum chamber. Beta, the ratio of plasma to magnetic field pressure is a measure of the efficiency of the utilization of the magnetic field and since the field and pressure fall off together,  $\beta$  only decays slowly with radius.

When a small uniform field is added in the direction of the dipole axis a separatrix will form which leads to two possible geometries: (1) When the uniform field adds to the outer dipole field the separatrix exhibits two symmetric nulls on the dipole axis as exhibited in Fig. 3. (2) When the uniform field subtracts from the outer dipole field the separatrix exhibits a field null on the outer midplane, as seen in Fig. 4. Within the last closed flux surface we expect to satisfy the MHD requirement  $\delta(pV) > 1$ . Outside the last closed flux surface the plasma will flow along field lines into the end wall.

Beyond the separatrix heat will be conducted along the field lines and flow toward the end plates or limiter. A strong fanning of the diverted field lines is expected to greatly reduce the end wall power density. The plasma at the divertor plates is expected to be 1 to 10 eV and at the symmetry point (opposite the end plate) 20 to 100 eV. As with a tokamak divertor the scrape-off layer plasma can be lead into a baffled chamber to permit pumping at high neutral pressure with a limited back streaming of the neutralized outflow.

One straightforward way to heat a laboratory dipole experiment would be to utilize electron cyclotron resonance heating (ECRH). For an ECRH heated experiment the heating will take place at both the fundamental and the second harmonic resonance field locations and the hot electrons will be localized between the flux surfaces that are tangent to the fundamental and the second harmonic mod-B surfaces. A typical laboratory embodiment of a levitated dipole could utilize 2.45 to 28 GC ECR heating. The coil design used in Fig. [1] is constrained by the current density limit for a superconductor, taken here to be  $1 \times 10^8$  A/m<sup>2</sup>, and by the requirement that the resonant flux tube clears the coil.

The vacuum field of a circular loop provides a useful analytic approximation. The vector potential for the field of a single loop of radius  $R_c$  in cylindrical coordinates has the form

$$A_\theta = \frac{\mu I}{\pi k} \left( \frac{R_c}{r} \right)^{1/2} [(1 - 0.5k^2)K(k^2) - E(k^2)], \quad (1)$$

with  $\mathbf{B} = \nabla \times \mathbf{A}$  and the magnetic flux surfaces are given by  $rA_\theta$ .  $\mathbf{K}$  and  $\mathbf{E}$  are complete elliptic integrals of the first and second kind. The ring current is  $I$  and

$$k^2 = \frac{4R_c r}{(R_c + r)^2 + z^2}.$$

For  $r \gg R_c$  the field has a dipole dependence

$$B(r, \theta) = \frac{\mu_0 M}{4\pi r^3} (1 + 3 \sin^2 \theta)^{1/2}. \quad (2)$$

An additional vertical field term,  $A_{\theta \perp} = 0.5B_\perp r$  term must be added to the vector potential (Eq. 1) to produce a diverted geometry.

### 3. SCRAPE-OFF LAYER CONSTRAINT

Since the pressure gradient must not exceed a critical value the peak pressure,  $p_0$ , is determined by the scrape-off layer pressure:

$$p_0/p_{sol} = (r_{sol}/r_0)^{20/3} \sim 10^5 - 10^7.$$

Assuming that a fraction  $f_R$  of power leaving the plasma is radiated we can balance the power loss from the plasma with the flow in the scrape-off layer:

$$\frac{(1 - f_R)p_0 V_0}{\tau_E} \approx 2p_{sol} A_{sol} c_s,$$

with  $c_s$  the scrape-off layer sound speed,  $V_0$  the effective volume of hot plasma defined by  $p_0 V_0 = \int p dV$ ,  $A_{sol}$  the scrape-off layer cross-section area and  $p_0$  ( $p_{sol}$ ) the respective core (scrape-off layer) pressures. The zero subscript denotes values at the location of the pressure peak. Assuming that the scrape-off layer width is a finite number of ion gyro radii, we take  $A_{sol} \approx \pi \gamma R_{sol} \rho_{sol}$  with  $\rho_{sol}$  the scrape-off layer ion gyro radius and  $\gamma$  the ratio of the scrape-off layer width to the ion gyro radius ( $\gamma \geq 1$ ). Taking  $V_0 \approx \pi R_0^3$  and imposing the critical temperature profile  $T \propto R^{-8/3}$  and  $\gamma = 1$  we obtain

$$\tau_E^{crit} \approx 0.5(1 - f_R) \frac{B_0 R_0^2}{\sqrt{T_{i0} T_{e0}}} \left( \frac{R_{sol}}{R_0} \right)^{16/3} \quad (3)$$

in MKS units with temperatures in eV. Consider two examples:

1. A dipole with  $R_0 = 0.4$  m,  $R_{sol} = 3$  m,  $B_0 = 0.4$  T,  $f_R = 0.5$ . For a hot electron plasma with  $T_{e0} = 300$  KeV,

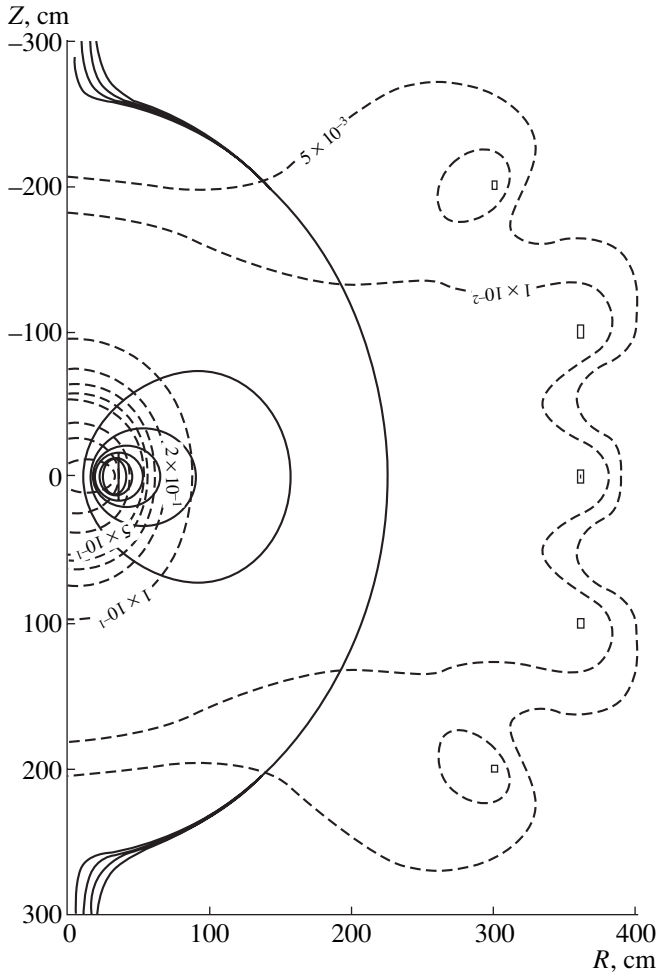


**Fig. 3.** Configuration with separatrix null points in dipole axis.

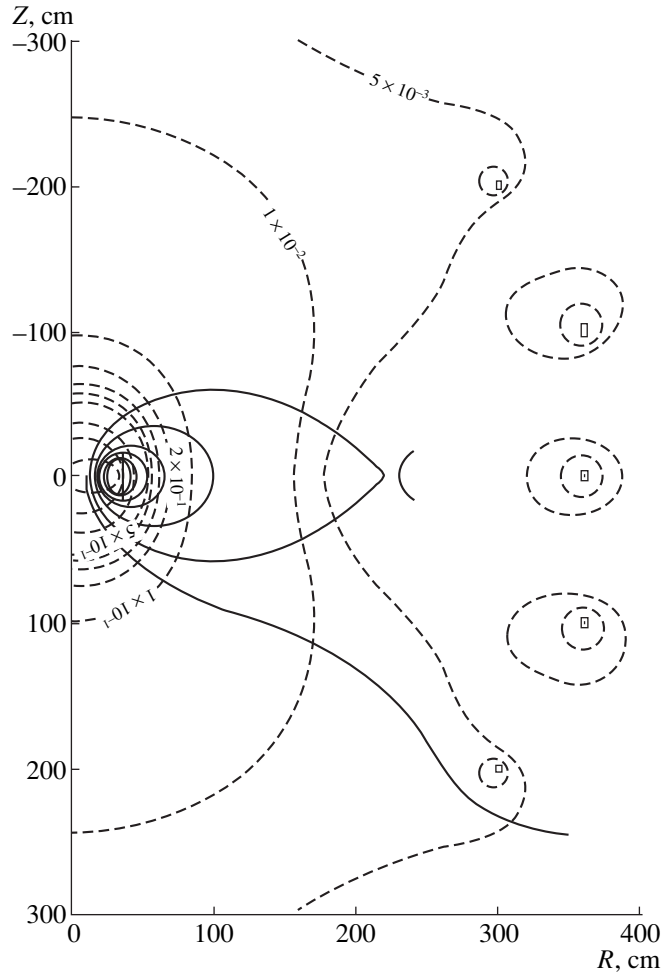


**Fig. 4.** Configuration with separatrix null on outer mid-plane.

and  $T_{i0} = 200$  eV, we obtain  $\tau_E \sim 0.1$  sec. For a density of  $n_e = 5 \times 10^{19} \text{ m}^{-3}$  this corresponds to  $\beta_e = 0.38$  and the power requirement of 75 KW. This estimate of power ignores the stabilization of the hot electron interchange mode by the thermal electron component [12] which would permit a higher ratio of peak to scrape-off layer pressure and thereby reduce the power requirements. Therefore this heating power estimate may be considered to be an upper bound.

2. For  $R_0 = 0.4$  m,  $R_{sol} = 3$  m,  $T_{i0} = T_{e0} = 5$  KeV,  $B_0 = 0.4$  T,  $f = 0.5$  we obtain  $\tau_E = 0.15$  sec. For a density of  $n_e = 2 \times 10^{19}$  this corresponds to  $\beta = 0.5$  and the power required to sustain this plasma is 65 KW.

For  $\tau_E < \tau_E^{crit}$  from (3) the scrape-off layer can expand to accommodate a higher heat flow, i.e.  $\gamma > 1$ . For  $\tau_E > \tau_E^{crit}$  the heating power must be decreased, i.e. the temperature  $T_0$  must decrease for the heating power to balance the scrape-off layer power outflow with the divertor width fixed at one ion gyro radius. This behav-

ior results from the constraint imposed by the adiabatic profiles of pressure and temperature.

We have assumed that  $T_{sol}/T_0 = (R_0/R_{sol})^{8/3}$ . More generally the temperature profile is determined by the heating and thermal transport profiles. The relationship of the temperature to the density profile is also constrained by stability considerations as discussed below. Furthermore the scrape-off layer temperature is determined by the cooling processes that take place within the scrape-off layer including radiation and secondary electron emission. As the plasma flows along the scrape-off layer field lines toward the end plates it will cool and it can become collisional. The scaling changes when the mean free path within the scrape-off layer becomes less than the connection length and the heat flow along the field lines becomes predominantly conductive. For a collisional plasma the temperature will vary along the field line in the scrape-off layer (at constant pressure) due to parallel thermal conductivity. Additionally if the neutral pressure becomes sufficiently large (in the vicinity of the end walls) the pres-

sure can fall due to momentum exchange with neutral particles.

For a collisional scrape-off layer the power balance becomes

$$\frac{(1 - f_R)p_0V_0}{\tau_E} \approx \frac{p_{sol}\chi_{\parallel}V_{sol}}{L_{sol}^2},$$

and we note that for classical conductivity  $\chi_{\parallel} \propto T^{7/2}$ . Since collisionality retards the outflow of heat along open field lines the scrape-off layer temperature can be higher without degrading core confinement as compared with a collisional scrape-off layer.

#### 4. MHD AND ELECTROSTATIC MODE STABILITY

The dipole reactor concept is based on the idea of generating pressure profiles near marginal stability for low-frequency MHD and electrostatic fluctuations. From ideal MHD, marginal stability results when the pressure profile,  $p(\psi)$  satisfies the adiabaticity condition,  $\delta(pV') = 0$ , where  $V$  is the specific flux tube volume and  $\gamma = 5/3$  [13]. Hasegawa pointed out that when the invariants  $\mu$  and  $J$  are conserved, marginal stability of both MHD and drift modes results when  $\partial F(\mu, J, \psi)/\partial \psi = 0$ , where  $F$  is the particle distribution function and  $\psi$  is the third adiabatic invariant. Both of these conditions lead to dipole pressure profiles that scale with radius as  $p \propto r^{-20/3}$ .

At high beta MHD ballooning is expected to provide a stability limit. The stability of ballooning modes has been studied for both magnetospheric and fusion dipole applications [14–15] and these studies indicate a beta limit in excess of  $\beta > 1$ . For application to planetary systems or for supported dipole experiments one must take account of anisotropic pressure and also the boundary conditions where the field lines enter the poles. For fusion applications one is interested in a levitated dipole which has closed field lines and therefore we expect the pressure to be isotropic. For an isotropic pressure we can apply the standard MHD formalism.

On the other hand, since confinement in a levitated dipole results from cross field transport, (and not pitch-angle scatter) it may be expected that, on a transport time scale, the distribution function will become isotropic. To lowest order the distribution function would be approximated by  $F_0 = F_0(\epsilon, \psi)$  with  $\epsilon = (v_{\perp}^2 + v_{\parallel}^2)/2$ , the particle energy. It still remains true that low frequency unstable modes ( $\omega \ll \omega_b, \Omega_c$ ) would lead non-linearly to the adiabatic distribution function,  $\partial F(\mu, J, \psi)/\partial \psi = 0$ . The subsequent collisional relaxation of the distribution function will preserve  $n$ ,  $T$ , and  $\eta$  ( $\eta \equiv d \ln T / d \ln n$ ) and this has important consequences for micro stability.

#### Interchange Modes from Kinetic Theory

When  $F_0 = F_0(\epsilon, \psi)$  the kinetic analysis of electrostatic drift modes proceeds from a traditional approach [16] beginning with the drift kinetic equation. A kinetic stability analysis of interchange modes produces similar results to the MHD interchange criterion. In [16] it is shown that, interchange modes become stable when the following criterion is satisfied:

$$\int d^3 v F_0 (\bar{\omega}_d^2 - \bar{\omega}_d \omega_*) > 0, \quad (4)$$

where  $\omega_* = \mathbf{b} \times \mathbf{k}_{\perp} \cdot \nabla F_0 / m \Omega_c F_{0e}$  is the diamagnetic drift frequency,  $\omega_d = \mathbf{k}_{\perp} \cdot \mathbf{b} \times (m v_{\parallel}^2 \mathbf{b} \cdot \nabla \mathbf{b} + \mu \nabla B) / m \Omega_c$  is the precessional drift frequency, and  $\mathbf{b} = \mathbf{B} / |\mathbf{B}|$ . In this analysis we have assumed  $\omega \ll \omega_b$  with  $\omega_b$  the bounce frequency defined by  $\omega_b = v_{\parallel} d/ds$  and we have bounce averaged the drift kinetic equation. The bounce averaged quantities appear with an overline,  $\bar{a} = \int a dl / v_{\parallel}$ . This yields the approximate stability criterion  $\omega_d > (1 + \eta) \omega_*$  which indicates that (at low  $\beta$ ) stability requires that the local pressure scale length exceeds the radius of curvature.

#### Trapped Particle Modes

Trapped particle modes are low frequency electrostatic modes ( $\omega \ll \omega_b \ll \Omega_c$ ) that can localize in the outer part of the torus. For a tokamak  $\omega_d / \omega_* \approx 1/A \ll 1$  and as a result we can ignore resonances with the precessional drift,  $\omega_d$ , and obtain drift frequency fluctuations of order  $\omega \sim \omega_*$ . With a dipole we have the opposite ordering, i.e.  $\omega_d / \omega_* > 1$  and stability of interchange modes require  $\omega_d > (1 + \eta) \omega_*$ . The dipole ordering leads to the result that instability may be driven by a resonance of the wave with the precessional drift motion, i.e.  $\omega \sim \omega_d$ .

An analysis of the dissipative trapped ion mode that assumes collisional electrons and collisionless ions indicates a stability criterion  $\omega_d > \eta \omega_* / 2$  [16]. Likewise an analysis of a collisionless trapped particle mode indicates a stability criterion  $\omega_d > \eta \omega_*$  [16]. Therefore we can conclude that, in a levitated dipole, a pressure profile that is stable to interchange modes may also be stable to trapped particle modes.

#### $\eta_i$ Modes

In a tokamak the so-called  $\eta_i$  or “mixing” modes are electrostatic modes that couple ion acoustic and drift fluctuations. They are low frequency modes  $\omega \ll \Omega_{ci}$  but include the dynamics of the bounce frequency time scale. A dipole does not have magnetic shear and so we will refer to the early derivations of the  $\eta_i$  mode which do not include magnetic shear. Antonsen *et al.* [17–18]

derives stability criteria from both a fluid and a collisionless kinetic theory. The simplest fluid theory indicates that instability occurs when  $\eta_i > 2/3$ . The adiabatic distribution is characterized  $\eta_i = \nabla \ln T_i / \nabla \ln n = 2/3$ . The more detailed fluid derivation and the collisionless kinetic approach indicate that instability occurs when  $\eta_i > 1$ . Thus adiabatic profiles which are characterized by  $\eta_i = 2/3$  are expected to be stable to these modes.

### *Drift Cyclotron Modes*

Drift cyclotron modes are high frequency unstable modes ( $\omega \sim \Omega_{ci}$ ) modes that are driven by temperature and density gradients. Pastukhov and Sokolov have evaluated the transport from these modes in the good curvature region near the surface of the levitated dipole [19, 20]. They show that the resulting transport would be severely limited by particle recycling at the surface of the internal coil. Because the surface of dipole is completely surrounded by a dense plasma, the net particle flux to the ring must vanish. A cool, high-density sheath forms at the dipole surface which transforms the thermal flux into bremsstrahlung radiation.

### *Stability of Convective Cells*

Experiments in multipoles have indicated that convective cells [21] can provide the dominant source of cross-field transport in shear-free systems. It is understood theoretically [22] that zero frequency convective cells are closely related to interchange modes and they will grow in regions of bad magnetic well, i.e. where  $\delta(pV') < 0$ . In addition it has been shown that convective cells will exist in regions of good curvature when the heating is non-uniform [23]. In the Wisconsin octopole experiments convective cells were observed in regions of both good and bad curvature [22] regions and the convective cells were observed to decay. In these experiments the initial plasma was non-uniformly distributed within the chamber. These experiments also indicated that a small amount of shear caused a rapid decay of the convective cells. Additionally it was observed that small field errors can cause convective flow patterns in a shear-free configuration [24].

These results lead one to suspect that uniform heating will be required in a levitated dipole in order to avoid the excitation of convective cells. Alternatively one can consider the addition of a small current on the dipole axis (or appropriate current drive) to create some shear and thereby eliminate these modes.

On the other hand, convective cells can be useful in a reactor to purge the ash. At marginal stability,  $pV' = \text{const}$ , the exchange of flux tubes will transport particles but not energy. Additionally when  $n_e \propto 1/V$  ( $\eta_i = 2/3$ ) the exchange of flux tubes will not change the density profiles. Therefore for an adiabatic profile the controlled application of asymmetric heating can provide a

means for the adiabatic convection of the fusion products. One might then consider the possibility that, in a reactor, a fraction of the synchrotron radiation that is emitted from the plasma can be reflected back so as to be non-uniformly reabsorbed and therefore drive convective cells that fuel and cleanse the plasma.

### *Conclusions on Stability*

In general the radial profiles of heating and fueling determine the respective temperature and density profiles. We can imagine heating and fueling profiles that generate marginally stable pressure profiles ( $p \propto V^{-\gamma}$ ) while maintaining  $\eta_i < 2/3$ . If we exceed the critical pressure gradient we would expect the plasma to expand unstably so as to broaden the pressure profile. If we exceed a critical value of  $\eta_i$  we would expect an onset of micro-turbulence drive transport. This is in direct analogy to the operation of a tokamak. With pressure gradients and  $\eta_i$  appropriately bounded a levitated dipole may exhibit classical transport.

## 5. ECR HEATING AND PELLET INJECTION

Electron cyclotron resonance heating provides a straight forward method to build up a substantial stored energy in a hot electron plasma. This capability results from the predicted stability at high beta and the closed field line geometry of a levitated dipole. The energy stored in the hot electron plasma can be transferred into a high density, thermal hydrogenic plasma by injecting pellets into the ECR heated hot electron plasma. The energy transfer into the hydrogenic and the thermal electron species depends on a competition between re-thermalization and radial thermal transport. If transport is classical or near classical essentially all of the stored energy can be transferred into the hydrogenic and the thermal electron species. In this optimistic scenario D<sup>3</sup>He ignition could be obtained in an inexpensive manner in a relatively small reactor.

If we consider, for example, a dipole plasma heated by a 28 GC gyrotron at the 1 T resonance surface (about 100–200 KW of power) we may expect to produce a hot electron plasma with  $n_e \sim 2\text{--}5 \times 10^{18} \text{ m}^{-3}$  at 200–500 KeV ( $0.2 < \beta < 1$ ). The ability to transfer the energy depends on the competition of cross field transport and thermalization of the hot electron energy. For classical confinement, a large fraction of the energy could be transferred and a  $n_e \sim 2 \times 10^{18} \text{ m}^{-3}$ , 200 KeV electron plasma would yield a 10 KeV hydrogenic plasma at  $n_e \sim 2 \times 10^{19} \text{ m}^{-3}$ .

To study this process we utilize a zero dimensional model assuming classical re-thermalization between the suprathreshold and the thermal species. Thermal plasma losses due to cross field transport characterized by  $\tau_E$  and  $\tau_P$ . We solve the following simultaneous rate

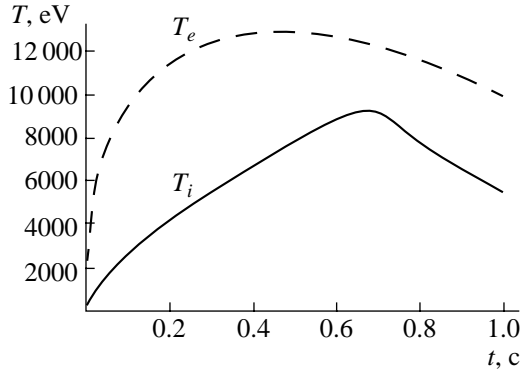


**Fig. 5.** Solution to rate equations for electron and ion temperatures with  $\tau_E = a^2/\chi_\perp$  for  $a = 0.1$  m, and initial values of  $n_{eh} = 5 \times 10^{18} \text{ m}^{-3}$ ,  $n_{i0} = 5 \times 10^{19} \text{ m}^{-3}$ .

equations for hot electrons,  $T_{eh}$ , thermal electrons,  $T_e$ , thermal ions,  $T_i$ , and density,  $n_e$  (assuming  $n_e = n_i$ ):

$$\begin{aligned} \frac{dT_{eh}}{dt} &= \frac{T_e - T_{eh}}{\tau_{ei}} + \frac{T_i - T_{eh}}{\tau_{ih}}, \\ \frac{dT_e}{dt} &= \frac{T_{eh} - T_e}{\tau_{ei}} + \frac{T_i - T_e}{\tau_{ei}} - \frac{T_e}{\tau_{Ee}}, \\ \frac{dT_i}{dt} &= \frac{T_{eh} - T_i}{\tau_{ih}} - \frac{T_i - T_e}{\tau_{ei}} - \frac{T_i}{\tau_{Ei}}, \\ \frac{dn_i}{dt} &= -\frac{n_i}{\tau_p}, \end{aligned}$$

with  $\tau_{ei}$  the classical rethermalization time,  $\tau_{ih}$  the hot electron-ion rethermalization time,  $\tau_{Ei}(\tau_{Ee})$  the ion (electron) energy confinement and  $\tau_p$  the particle confinement time. The energy confinement time is related to a mean transport coefficient by  $\tau_E \approx \delta^2/4\chi$ .

For classical confinement essentially all of the energy can be transferred into the thermal plasma. One example would be to consider classical confinement with  $\tau_E = a^2/\chi_\perp$  for  $a = 0.1$  m and initial values of  $n_{eh} = 5 \times 10^{18} \text{ m}^{-3}$ ,  $n_{i0} = 5 \times 10^{19} \text{ m}^{-3}$ . As shown in Fig. 5  $T_e$  rises up to 12 KeV and  $T_i$  reaches 8 KeV. A second example, shown in Fig. 6 shows the solution to rate equations for with  $\tau_E = 20$  ms  $\tau_p = 200$  ms and  $a = 0.1$  m. Even for substantially reduced ion confinement significant plasma parameters would be attained due to energy transfer from the relativistic electrons. Thus, by combining ECRH and pellet injection a modest dipole experiment might be capable of investigating the properties of high temperature, high density, and high beta plasmas.

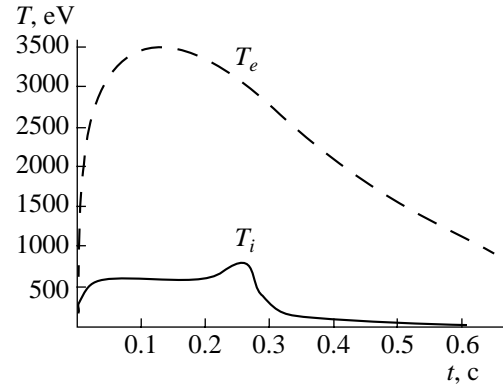


**Fig. 6.** Solution to rate equations for electron and ion temperatures with  $\tau_E = 20$  ms,  $\tau_p = 200$  ms and  $a = 0.1$  m.

## 6. THERMAL EQUILIBRIA OF AN IGNITED D<sup>3</sup>HE PLASMA

An estimate of the equilibrium profiles in an ignited D<sup>3</sup>He plasma requires a solution of a heat transport equation. This is a two-dimensional problem since the magnetic field strength varies along a field line (the density and temperature are flux functions) In a levitated dipole geometry a major portion of the volume of confined plasma is located near the outer midplane. We can therefore estimate confinement using a one dimensional model that uses fields evaluated at the outer midplane of the dipole. We assume D<sup>3</sup>He power production with a 20% D, 80% 3He mixture and furthermore assume that the dominant loss channels are Bremsstrahlung radiation and classical transport. The magnetic field also enters the Jacobian to describe the flux tube expansion and for classical transport  $\kappa_\perp \propto 1/B^2$ . We can write the thermal transport equation in flux coordinates using the magnetic scalar potential,  $\chi$ , as the angular coordinate, i.e.  $\mathbf{B} = \nabla\chi$ . The flux tube average of the transport equation then gives:

$$\begin{aligned} \frac{\partial}{\partial \psi} n(\psi) \left[ \int \partial \chi R^2 \kappa_\perp \right] \frac{\partial T}{\partial \psi} \\ = [n_D n_{He} \langle \sigma v \rangle_{D^3He} E_{fus}(T) - P_{brem}(T)] \int \frac{d\chi}{B^2}. \end{aligned} \quad (5)$$

On the right hand side  $\langle \sigma v \rangle_{D^3He}$  is the D<sup>3</sup>He rate coefficient,  $E_{fus} = 18.3$  MeV and  $P_{brem}$  is the Bremsstrahlung radiation power given in [25]:

$$\begin{aligned} P_{brem} = 5 \times 10^{-37} \sqrt{T} n_e^2 [Z_{eff}^2 (1 + 1.55 \times 10^{-3} T_e \\ + 7.15 \times 10^{-6} T_e^2) + 0.071 (\sum Z_i^3 n_i/n_e) T_e^{-1/2} \\ + 0.00414 T_e] \end{aligned}$$

in  $\text{W/m}^3$  with  $T$  in KeV and  $n_e$  in  $\text{m}^{-3}$ . On the dipole midplane  $R = R_0$  and (4) becomes:

$$\frac{1}{R_0 B_0} \frac{\partial}{\partial R_0} n_e \kappa_{\perp 0} \frac{B_0}{R_0} \left[ \int \frac{\partial l}{B} R^2 \right] \frac{\partial T}{\partial R_0} \quad (6)$$

$$= [n_D n_{\text{He}} \langle \sigma v \rangle_{\text{DHe}^3} E_{fus}(T) - P_{brem}(T)] \int \frac{dl}{B}.$$

We have used  $\kappa_{\perp} \propto 1/B^2$  i.e. we have assumed classical transport.

The flux average integrals, can be approximated by  $\int (dl/B) R^2 \propto R_0^6$  and  $\int (dl/B) \propto R_0^4$ . The scaling of (5) indicates that the temperature half-width,  $\Delta_T$  scales as  $\Delta_T \propto \sqrt{\kappa_{\perp}/H(T)}$  with  $H(T)$  the sum of the heating terms from the right hand side of (5) Therefore a larger thermal transport leads to a broader temperature profile. If we compare the total heat flux toward the ring vs toward the scrape-off-layer we can show that when  $\Delta_T \ll R_{0T}$  with  $R_{0T}$  the location of the temperature peak. The ratio of heat to the ring vs heat to the scrape-off-layer is  $H_R/H_{sol} \approx 1 + 6\Delta_T/R_{0T}$ .

To solve Eq. (6) a density dependence must be assigned but since all terms go as  $n^2$  this dependence only has a weak effect on the solution. (The pressure gradient, however, enters into the stability criteria and the pressure gradient broadens when the density profile broadens). The solution of (5) is a strong function the amplitude and radial dependence of  $\kappa_{\perp}$  which we have taken to be classical. Thus at a fixed beta, as the magnetic field increases the peak fusion power density rises as  $B^2$  but additionally the hot plasma region narrows due to reduced transport.

## 7. DISCUSSION

A dipole fusion reactor would consist of a single levitated circular magnet within a large vacuum chamber. The hot plasma core would encircle the levitated dipole coil forming a toroidal annulus. A large expansion region of cooler plasma extends outward from the dipole where the plasma pressure decreases with radius,  $R$ , approximately as  $R^{20/3}$  characteristic of the marginally stable profiles found in magnetospheres. Although the overall dimensions of the dipole fusion reactor may be large, the size of superconducting dipole magnet is small. Indeed, in the dipole reactor conceptual designs [3–5] the volume of the hot plasma core ( $40 \text{ m}^3$ ) exceeds the volume of the levitated ring ( $20 \text{ m}^3$ ). This feature of the dipole reactor (i.e. a larger plasma volume than the volume of the high-technology superconducting magnets, shield and structure) is in sharp contrast to the tokamak where the volume of the plasma is usually less than the volume of the surrounding fusion island. (For example, in ITER, the plasma volume is  $2500 \text{ m}^3$  and the volume of the magnets,

shield and structure exceeds  $5000 \text{ m}^3$ ). The dipole reactor concept also differs from the spherator [26] since the plasma profiles of the spherator are steep (i.e. they cannot be made stationary) and low-frequency fluctuations or convection cells may significantly degrade confinement.

Conceptual dipole reactor designs have been reported [3–4], and the use a dipole fusion reactor for space propulsion has been proposed [5]. In each of these designs, D– $^3\text{He}$  fuel was used instead of the more highly reactive D–T fuel in order to reduce the neutron flux to the levitated coil. Also reflectors were used to reduce synchrotron losses from the high-pressure and lower  $\beta$  plasma on the inside of the levitated dipole. The high  $\beta$  capability of the dipole reactor makes possible the use of advanced and possibly aneutronic fuels, but the high temperatures required to burn these fuels necessitate steps to reduce synchrotron emission losses. The designs reported in [3] and [4] described compact and relatively low-power dipole reactors with large plasma expansion regions. A 20 MA dipole coil of radius of 1.8 m confined a plasma with peak  $\beta \sim 3$  and generated 100 MW of fusion power. A higher field, 40 MA dipole with a denser plasma at the same  $\beta$  could generate 1000 MW. The plasma is heated to ignition with direct heating of the plasma core (using, for example, neutral beam injection). In [5], a much larger dipole reactor containing a 54 MA dipole having a radius of 6 m and producing 2000 MW of fusion power was considered for rocket propulsion. The plasma expansion region was not as large and a relatively hot plasma was diverted to an annular gas-neutralizer to generate thrust. In both [4] and [5], thermoelectric converters were located within the levitated dipole, and they provided the power to drive refrigerators for the superconducting magnets. Designs of the superconducting magnets and shields in [3] and [5] illustrate the feasibility of reactor-sized dipole magnets using present-day multi-filamentary  $\text{Nb}_3\text{Sn}$  conductors.

Closely related studies of plasma confinement in multipole fields have been a subject of significant research efforts [27, 28]. Recent theoretical work includes the study of the equilibrium of two dimensional internal coil configurations [27–30].

Finally, a supported dipole laboratory experiment at Columbia University has studied the detailed phase-space evolution of dipole-trapped energetic plasma in the presence of intense drift-resonant fluctuations [9–10]. In this experiment, an ‘‘artificial radiation belt’’ (a population of 5–50 KeV energetic electrons) is produced with microwave heating which excites hot-electron interchange instabilities when the pressure gradient sufficiently exceeds the marginally stable profiles envisioned for the dipole reactor. Fluctuations leading to global chaotic transport as well as thin, localized regions of stochastic drifts are observed, and these observations have been used to verify models of collisionless radial transport in dipole magnetic fields.

## REFERENCES

1. Hasegawa, A., *Comments on Plasma Physics and Controlled Fusion*, 1987, vol. 1, p. 147.
2. Vampola, A.L., *Symp. on Natural and Manmade Rad. in Space*, (Wash., D.C.), 1972, p. 538.
3. Hasegawa, A., Chen, L., and Mauel, M., *Nuclear Fus.*, 1990, vol. 30, p. 2405.
4. Hasegawa, A., Chen, L., Mauel, M., Warren, H., Murakami, S., *Fus Tech.*, 1992, vol. 22, p. 27.
5. Teller, E., Glass, A., Fowler T.K., *et al.*, *Fusion Technology*, 1992, vol. 22, p. 82.
6. Dawson, J.M., *Private Communication*. See [5].
7. Mauel, M., Warren, H., Hasegawa, A., *IEEE Transactions on Plasma Science*, 1992, vol. 20, p. 626.
8. Mauel, M.E., Hasegawa, A., in *Physics of Space Plasmas*, Cambridge Scientific Pubs., 1990, p. 461.
9. Warren, H.P. and Mauel, M.E., *Phys. Rev. Lett.*, 1995, vol. 74, p. 1351.
10. Warren, H.P. and Mauel, M.E., *Phys. Plasmas*, 1995, vol. 2, p. 4185.
11. Sackett, S., "EFFI Electromagnetic Field Code", *LLNL Report UCRL-52402*, 1978.
12. Berk, H.L., *Phys. Fluids*, 1966, vol. 19, p. 1275.
13. Rosenbluth, M.N. and Longmire, *Ann. Phys.*, 1957, vol. 1, p. 120.
14. Hameiri, E., *et al.*, *J. Geophys. Res.*, 1991, vol. 96, p. 1513.
15. Chan, A., Xia, M., and Chell, L., *J. Geophys. Res.*, 1994, vol. 99, p. 17351.
16. Kesner, J., *Phys. Plasmas*, 1997, vol. 4, p. 419.
17. Coppi, B., Rosenbluth, M., Sagdeev, R., *Phys. Fluids*, 1967, vol. 10, p. 582.
18. Antonsen, T., Coppi, B., Englade, R., *Nuc. Fus.*, 1979, vol. 19, p. 641.
19. Pastukhov, V. and Sokolov, A.Yu., *Nuc. Fusion*, 1992, vol. 32, p. 1725.
20. Sokolov, A.Yu., *Plasma Phys. Rep.*, 1993, vol. 19, p. 1454.
21. Dawson, J.M., Okuda, H., and Carlile, R., *Phys. Rev. Lett.*, 1971, vol. 27, p. 491.
22. Hassam, A. and Kulsrud, R., *Phys Plasmas*, 1979, vol. 22, p. 2097.
23. Hassam, A., private communication, 1997.
24. Jernigan, T., Rudmin, J., and Meade, D., *PRL*, 1971, vol. 26, p. 1298.
25. McNally, J.R., *Nuclear Technology/Fusion*, 1982, vol. 2, p. 9.
26. Freeman, *et al.*, "Confinement of plasmas in the spherator", in *Proc. 4th Conf. Plasma Physics and Controlled Nuclear Fusion*, Madison, Wisconsin, June 17-23, 1971, IAEA-CN-28/A-3, vol. 1, p. 27.
27. Ohkawa, T. and Kerst, D.W., *Nuovo Cimento*, 1961, vol. 22, p. 784.
28. Navratil, G., Post, R.S., and Butcher Ehrhardt, A., *Phys Fluids*, 1977, vol. 20, p. 157.
29. Maikov, A.R., Morozov, A.I., and Sveshnikov, A.G., *Plasma Physics Reports*, 1996, vol. 22, p. 87.
30. Morozov, A.I. and Murzina, M.B., *Plasma Physics Reports*, 1996, vol. 22, p. 500.

bremsstrahlung  
usefill